18th Australasian Fluid Mechanics Conference
Launceston, Australia
3-7 December 2012

Numerical Simulation of Spheres in Relative Motion Using Dynamic Meshing Techniques

Z.Q. Leong[1], D. Ranmuthugala[2], I. Penesis[1] and H.D. Nguyen[1]

[1]National Centre for Maritime Engineering and Hydrodynamics
Australian Maritime College, University of Tasmania, Launceston, 7248, Australia

[2]National Centre for Ports and Shipping
Australian Maritime College, University of Tasmania, Launceston, 7248, Australia

Abstract

The commercial Computational Fluid Dynamics (CFD) code *ANSYS CFX* was used to simulate the flow around three dissimilar spheres in relative motion over a large range of Reynolds numbers (R_e) from 10^2 to 10^6. The simulations utilise a six degrees-of-freedom Rigid Body Dynamics (RBD) solver to predict the motion of spheres in response to external forces. The simulations were intended to provide a benchmark of the code in its ability to accurately predict the flow around multiple submerged bodies, such as submarines and unmanned underwater vehicles (UUV) in relative motion. The simulations were found to be in good agreement with both experimental data for the drag predictions and analytical solutions for the simulated motions.

Due to the large relative motions between the spheres, the CFD simulation domain undergoes significant deformation, requiring dynamic meshing techniques to maintain the integrity of the mesh and solution. A number of options including mesh deformation and adaptive re-meshing, immersed solids, turbulence models, and the interface with the RBD solver were evaluated to optimise the time and resource utilisation, while maintaining acceptable accuracy and stability. The study identifies the merits of the different options to simulate multiple bodies in relative motion and provide time dependent hydrodynamic data at sufficient accuracy and speed to enable dynamic coupling with a control system for manoeuvring simulation of underwater vehicles.

Nomenclature

Symbol	Description	Equation
A_c	Characteristic Area (m^2)	$\pi D^2/4$
C_D	Drag coefficient	$2F_D/(\rho U^2 A_c)$
F_D	Drag force (N)	
ρ	Fluid density (kg/m^3)	
υ	Fluid kinematic viscosity (m^2/s)	
U	Freestream velocity (m/s)	
N	Net force of weight and buoyancy (N)	$mg - V\rho$
R_e	Reynolds number	UD/υ
m_a	Sphere estimated added mass (kg)	$(2/3)\pi(D/2)^3\rho$
$\ddot{z}$	Sphere acceleration (m/s^2)	
$\ddot{z}_a$	Sphere analytical acceleration (m/s^2)	$N(m+m_a)$
dz_a	Sphere analytical displacement (m)	$0.5N(m+m_a)t^2$
dz	Sphere displacement (m)	
D	Sphere diameter (m)	
m	Sphere mass (kg)	
V	Sphere volume (m^3)	$(4/3)\pi(D/2)^3$

Introduction

When an UUV is operating in proximity to a larger vessel, interaction with the wake and pressure field generated by the latter can impose rapid acceleration changes on the UUV. This can cause the vehicle to undergo uncontrollable oscillations which in extreme cases can result in collision or loss of the vehicle. Therefore, it is important for designers to have a good understanding of the vehicle's behaviour under the effects of the interaction. This will enable designers to: develop control systems that are sufficiently robust enough to deal with the changes in acceleration, improve the hydrodynamic performance of the vehicle, and establish safe operating envelopes.

In general, the hydrodynamic characteristics of underwater vehicles can be evaluated and quantified through experimental and empirical methods such as captive model testing and actual vehicle trials. However, these methods require considerable cost and time, and are restricted by the availability of suitable physical models of the vehicles and appropriate test facilities. For multi-body investigations the cost can increase up to three times that for a single body due to the complexities involved in the experimental setup [1].

Ongoing development of high performance computing facilities and numerical codes to predict fluid flow and pressure fields has enabled computer based simulations using CFD to replicate conditions that are difficult or costly to achieve through experimental processes. One of the major challenges faced when using CFD as an analysis tool for hydrodynamics is that computational results can vary greatly depending on the experience of the analyst, the setting utilised such as the boundary condition and the turbulence models, and the quality of the mesh grid. However, by combining both computational and experimental work, a validated simulation model could be obtained and used with confidence over the wider analysis range. This approach would be a more cost effective, faster, and viable alternative compared to one that is purely dependent on experimental work.

The flow past a sphere was chosen as a starting point for this study as there is extensive literature on its characteristics. Most numerical investigations on fluid flow around a sphere have been focused on using higher order schemes such as *Large Eddy Simulation* (LES) and *Direct Numerical Simulation* (DNS). These schemes have produced high quality and accurate predictions of the wake structure, shedding frequencies, and forces associated with a flow within a R_e range between 10^2 and 10^6 [2, 3]. Despite extensive numerical studies on sphere

hydrodynamics, there appears to be limited work using *Reynolds-Averaged Navier-Stokes* (RANS) simulations.

In RANS simulation, all scales of turbulence are modelled and the transport equations are represented in mean flow quantities. Although, this approach is less accurate for time dependent flow phenomena, e.g. vortex shedding, it offers a viable means to obtain reasonably accurate hydrodynamic forces acting on a submerged body in motion at greatly reduced computational effort. The reduction in mesh requirements for RANS simulation can be up to 10^3 orders of magnitude compared to an LES mesh of ~10^9 cells for equivalent accuracy [4]. In addition, the required time step for stability in RANS is determined by the fluctuation in the mean flow rather than turbulence. This allows RANS simulation to be carried out at time step of up to 100 times coarser than LES, especially for transient simulation with turbulent flows.

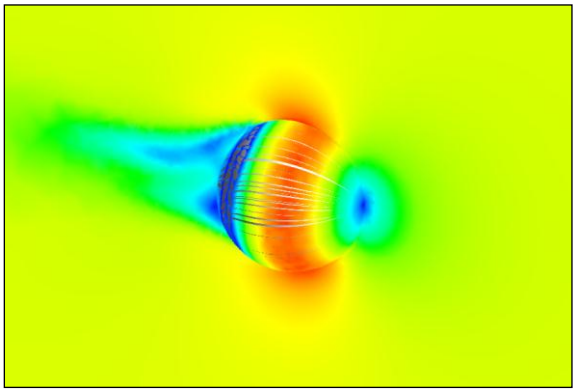

Figure 1. CFD visualisation of the velocity field and streamlines around a sphere in motion.

In this study, two dynamic mesh techniques, Mesh Deformation and Adaptive Re-meshing Method (MDARM) and Immersed Solid Method (ISM) are evaluated in terms of accuracy and computational speed for modelling fluid flow around a single smooth sphere in motion over a R_e range of 10^2 to 10^6. The MDARM simulations (see figure 1) were carried out with the *Shear Stress Transport k-omega* (SST) and *Baseline Reynolds Stress Model* (BSLRSM) turbulences models in addition to a laminar flow model providing a baseline for computational speed comparison. The ISM simulations were carried out with the SST model. The computational results were compared to experimental data to benchmark their accuracy. Coupled simulations of the flow and RBD solvers were also carried out to investigate the accuracy of the motion predictions compared to analytical solutions for three spheres in relative motion. The aim of the study was to establish which combination of turbulence model and dynamic meshing technique offered an efficient trade-off between accuracy and computational speed.

Numerical Model

Single Sphere Model

The three-dimensional (3D) computational domain is presented in figure 2. The size of the domain was 10m long, 2m wide and 2m deep. The diameter of the sphere was 0.1m. The sphere was located at an initial position 2m forward of the Outlet boundary and 1m away from the Farfield boundaries to ensure the pressure field generated by the sphere was well within the computational domain.

The MDARM simulations were carried out on an unstructured mesh containing 5.9×10^5 cells, made up of tetrahedrons in the regions away from the sphere and prisms around the sphere to capture the boundary layer as shown in figure 3. The sphere resides in a subdomain which allows the mesh within subdomain to be rigid, with deformation occurring only in the outer fluid domain. The mesh was progressively refined by subdividing the cells of the sphere surface and subdomain to examine the sensitivity of the drag predictions to the mesh density. At 7×10^6 cells, the variation in the predicted mean drag of the sphere was 6% compared to the 5.9×10^5 mesh cells model with the SST model at $R_e = 10^6$. Therefore, the latter mesh model was deemed sufficiently mesh independent with an uncertainty of 12% (2×6%). Further refining the mesh would result in the simulations being too expensive for coupling with a control system, as a smaller time step is required for smaller cells in order to satisfy the *Courant-Friedrichs-Lewy* (CFL) numbers of below 10 across the domain.

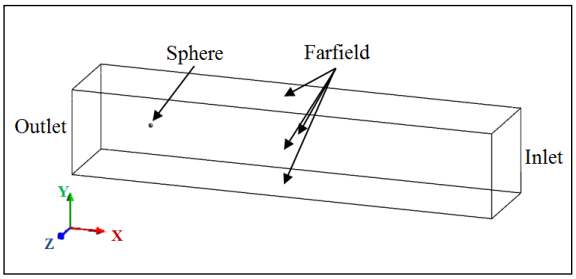

Figure 2. The single sphere computational domain.

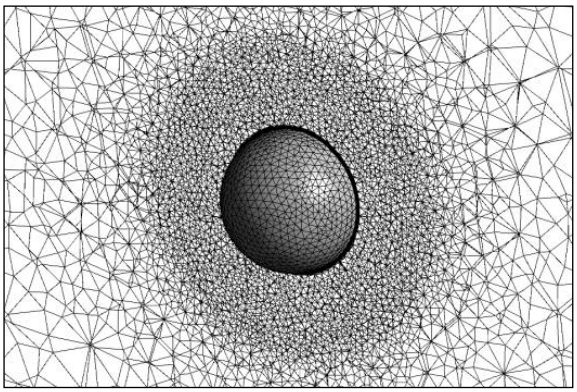

Figure 3. The MDARM mesh model.

For the evaluation of the ISMs simulations, the mesh for the sphere and fluid domain were individually generated and then overset as shown in figure 4. The mesh model of the sphere consists of the inner volume which requires only good mesh resolution on the sphere surface, e.g. mesh surface area error of less than 1%. The volume mesh inside the sphere may be arbitrarily coarse. The fluid mesh cells in which the sphere travels were refined to half the sphere surface mesh size to ensure two fluid domain nodes to every sphere domain node exist at the boundaries where the two domains intersect. This is required to ensure stability and smooth interpolation between the nodes of the fluid domain and the sphere. The result is a mesh model of approximately 7×10^6 cells.

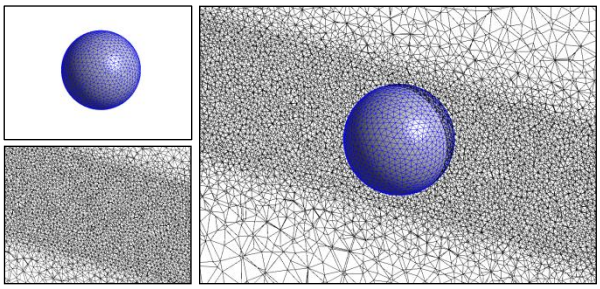

Figure 4. The ISM mesh model; sphere mesh (upper left), fluid domain mesh (bottom left).

Two Spheres Model

Two spheres with a diameter 0.1m were located within a computational domain size of 3m long, 2m wide, and 12m deep as shown in figure 5. The initial locations of the spheres were at z = -10m, 1m apart from each other, and 1m away from the Farfield boundaries. The mesh setup of the spheres was identical to the single sphere MDARM model. The mesh size was approximately 1.2×10^6 cells.

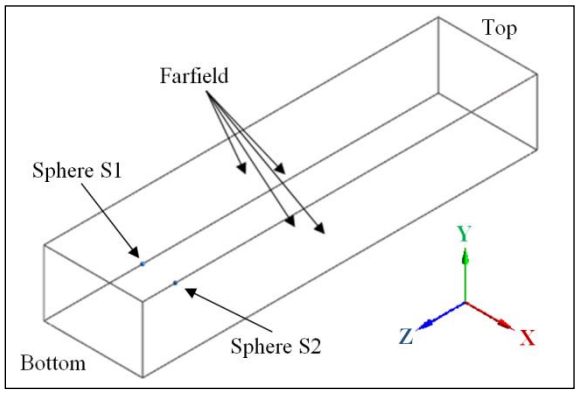

Figure 5. The two spheres computational domain.

Numerical Simulation

The simulations were performed using the CFD code *ANSYS CFX v14*, which uses a control volume based finite element discretization scheme. A time step between 0.1ms-1ms was used throughout the simulations in order to provide reasonably good time resolution of the forces and motions while maintaining CFL numbers of below 10 in the majority of the computational domain. The density and kinematic viscosity of the fluid were $997 kg/m^{-3}$ and $8.899\times10^{-4} m^2/s$ respectively.

Single Sphere Simulations

The essential aspect of the MDARM is that the mesh in the fluid domain deforms locally around the sphere as it moves and remeshes when the mesh quality is deemed compromised in terms of accuracy and stability. This overcomes the limited motions imposed by using a pure mesh deformation approach. Although mesh deformation is fully supported in *ANSYS CFX*, the re-meshing component is a *beta* feature and requires the use of a user-defined script. The latter, triggered by the mesh quality criterion, interrupts the simulation and transfers the positional state of the sphere into *ANSYS Workbench* in order to update the geometry and the mesh. The script then transfers the new mesh into the solver where the simulation information from the previous mesh is interpolated into the new mesh and the simulation is resumed. The mesh quality criterion was defined as the orthogonality angle in the mesh cells of no less than 10°.

For the ISM simulations, the sphere is defined as an immersed solid. As the sphere moves within the fluid domain, the velocity of the fluid nodes is enforced to be same as the velocity of the sphere by applying a set of source terms in the regions where the sphere mesh overlaps the fluid domain mesh. This method essentially avoids any mesh deformation, therefore remeshing is not required. The simulations were carried out with the SST turbulence model to model the turbulence in the freestream and the regions affected by the pressure field of the sphere. The ISM method does not resolve the boundary layer due to the inability to apply a wall treatment on the surface of the sphere.

Two Spheres Motion Response Simulation

For the motion response simulation, the flow solver was coupled with the RBD solver using the MDARM for modelling the relative motion between spheres. The spheres were submerged at an initial depth of 10m and were allowed to rise up freely. Different mass values were defined for each of the spheres, with the motion of each sphere dictated by the net force of its weight and buoyancy. The properties of the spheres are outlined in table 1.

Sphere	S1	S2
Mass, *m* [kg]	4.568E-1	3.915E-1

Table 1. Properties of the spheres for the motion response simulation

Results and Discussion

Figure 6 shows the mean drag coefficient (C_D) predictions of the MDARM simulations with SST, BSLRSM and Laminar model and the ISM simulations with SST against the experimental results by Schlichting [5].

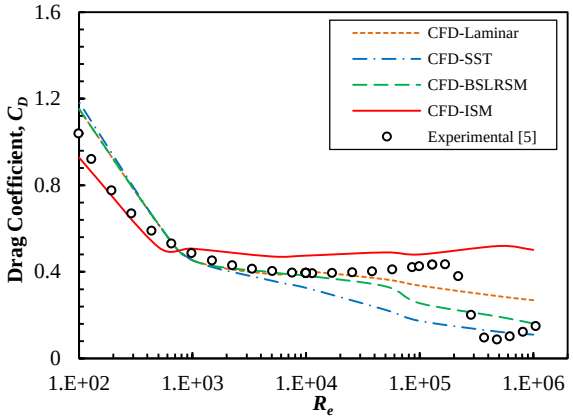

Figure 6. Mean drag coefficient of the single smooth sphere as a function of R_e.

At $R_e < 10^3$, where the flow around the sphere is below the turbulence wake regime, the ISM and the MDARM predictions compares favourably with the experimental results. The predictions of the MDARM-SST model and MDARM-BSLRSM were within 5% of the Laminar model. Although this is counterintuitive when turbulence models are applied for laminar flow since the boundary layer is modelled to be fully turbulent, the SST and BSLRSM are able to handle very small turbulence kinetic energy in the flow field thus able to give similar predictions to the Laminar model within the regime.

At $10^3 < R_e < 10^4$, the wake behind the sphere changes from laminar to turbulent, while its boundary layer remains laminar. The drag predictions of all models were in good agreement as shown in figure 6. At $R_e = 10^4$, the MDARM-SST model increasingly underpredicts the sphere drag as *Re* increases. The same was observed for the MDARM-BSLRSM drag predictions at R_e ~6×10^4 onwards. This is possibly due to the models overpredicting the turbulence kinetic energy in the sphere boundary layer thus pushing its separation further back. The predictions of MDARM-Laminar model and the ISM-SST model were found to be in good agreement with experimental results. It is noted that the predicted mean drag coefficient by the ISM-SST model remains around 0.5 as R_e increases thereafter.

At $10^5 < R_e < 10^6$, the flow in sphere boundary layer transitions from laminar to turbulent causing a sudden drop in drag which is commonly referred as the 'drag crisis'. None of the models were able capture the drag crisis characteristics. This was expected as none of the models were designed for transitional flows. However, the MDARM used with turbulence models were able to exhibit a gradual decline in drag within the regime and gave good predictions when the flow was fully turbulent at $R_e = 10^6$. Both the MDARM-Laminar and ISM-SST models were unable to accurately predict the drag on the sphere for turbulent boundary layer dependent flow.

The MDARM simulations were carried out with 6 core processers, and the ISM simulations 16 core processers due to its high mesh density. Table 2 outlines the computational effort of the simulations at $R_e = 10^6$. The time for each re-meshing event in the MDARM simulations was approximately 50 seconds. Although the MDARM-Laminar required the least computational effort, the model was insufficiently accurate for flow speeds where turbulence is prevalent. The MDARM-BSLRSM drag prediction was the most accurate, 11% closer to experimental results compared to MDARM-SST, however, the former required 42% more computation effort. Therefore, the MDARM-SST model was reasoned to be the most efficient in terms of accuracy and computational speed. The ISM was the most computational expensive option in both mesh requirement and computational time. Although the ISM does not require re-meshing, the advantage was offset by the fine mesh required in regions where the sphere travels to maintain simulation stability resulting in a substantial increase in mesh density. The ISM is more suited for simulations of bodies undergoing localised rotational motion or medium displacement.

Model	Mesh Cells	Time per inner loop [s]	Effort compared to MDARM-Laminar
MDARM-Laminar	6×10^5	24	1.00
MDARM-SST	6×10^5	29	1.20
MDARM-BSLRSM	6×10^5	41	1.70
ISM-SST	7×10^6	400	194

Table 2. Computational effort of the simulations at $R_e = 10^6$.

Two Spheres Results

The simulation results for the linear acceleration of the spheres, were found to be in good agreement with the analytical solution, $\ddot{z}_a$, which was based on Newton's second law of motion,. The simulation result for the linear acceleration of S1 was 0.866m/s^2 while the analytical result was 0.892m/s^2, giving an error of 3%. For S2, the simulation result was 1.803m/s^2 with the analytical result being 1.962m/s^2, giving an error of 8%.

Figure 7 shows the simulation results for the *z*-displacement of the two spheres plotted in comparison to the analytical results. The analytical results were obtained by twice integrating $\ddot{z}_a$ with respect to time. The simulation results underpredicted the motions compared to the analytical results but were within 10% of the latter. This was considered acceptable as the analytical results did not take into account the fluid drag acting on the spheres.

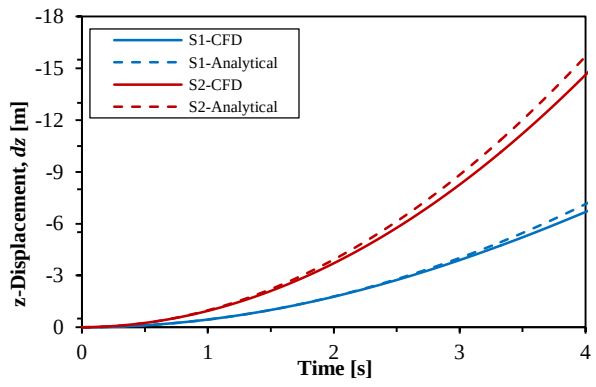

Figure 8. The *z*-displacements of the two spheres.

Conclusions

The present work is directed towards developing a simulation environment of an underwater vehicle manoeuvring in relative motion to a larger vessel, with the extensibility for coupling with the vehicle's control system. The simulation model needs to provide time dependent hydrodynamic data of reasonable accuracy and sufficient speed to enable efficient coupling with the control system for manoeuvring simulations of underwater vehicles.

The performance of RANS-based simulations with and without turbulence models, coupled with the dynamic mesh techniques, to simulate the fluid flow around a sphere undergoing large displacements within $10^2 < R_e < 10^6$ were examined. The MDARM-SST model was the most efficient in terms accuracy and computational speed with the drag predictions of the model being in good agreement with experimental data, except for within the flow regime where the sphere boundary layer changes from laminar to turbulence. The MDARM-BSLRSM predictions were 11% closer to experiment at fully turbulent flow at $R_e = 10^6$ compared to the SST model but took 42% more computational time.

The MDARM was found to be far superior for modelling bodies with large displacement compared to the ISM in both accuracy and computational effort. Although the ISM does not require re-meshing or a mesh to resolve the boundary layer around each body, it still requires a fine mesh in the fluid domain regions where the body travels. This fine mesh increases substantially with the motion range thus also increasing computational time. In addition, the inability of the ISM to model the boundary layer accurately has shown to give poor drag predictions at higher flow speeds. The motion predictions of the coupled flow solver and RBD solver simulations for two spheres in relative motion were found to be in good agreement to analytical solutions.

Currently, work is being carried out to model a 6-DOF UUV and a larger submerged vessel in relative motion, which requires simulation of the vehicle's hydrodynamic behaviour close to the larger vessel. The simulation model is also being improved to provide faster real time data linked to a MATLAB-based control environment replicating the UUV's control algorithm. In conjunction with the numerical work, experimental model tests are being carried out to validate the capability of the simulation to predict the hydrodynamic interaction between the UUV and the larger vessel.

References

[1] Park, J.Y., Jun, B.H, Lee, P.M & Oh, J., Development of test-bed AUV ISiMI and underwater experiments on free running and vision guided docking, *Underwater Vehicles*, I-Tesh, 2008.

[2] Jones, D.A. & Clarke, D.B., *Simulation of Flow past a Sphere using the Fluent Code*, Defence Science and Technology Organisation, 2008.

[3] Beratlis, N., Squires, K. & Balaras, E., Numerical investigation of Magnus effect on dimpled spheres, *Journal of Turbulence*, **13**, 2012, 1-15.

[4] Menter, F.R., *Turbulence Modelling for Engineering Flows*, ANSYS, Inc., 2012.

[5] Schlichting, H., *Boundary-Layer Theory*, New York, McGraw-Hill, 1979.